Coupled oscillations of double-walled carbon nanotubes

Giacomo Po[a] and N. M. Ghoniem[a]
Department of Mechanical and Aerospace Engineering, University of California, Los Angeles (UCLA), Los Angeles, California 91344, USA

(Received 17 December 2009; accepted 6 February 2010; published online 6 May 2010)

A study of the coupled axial and angular oscillations of double-walled carbon nanotubes (DWNTs) was performed using molecular dynamics simulations. In order to determine the oscillation frequencies inner and outer shells have been assumed to behave as rigid bodies, a 6–12 Lennard–Jones potential was used to model the van der Waals forces between them, and friction was neglected. Armchair (5, 5)/(10, 10) configurations, with tube lengths in the range of 25–1000 Å were investigated. The axial oscillation frequency was found to be a decreasing function of the DWNT length L (~78 GHz for $L=25$ Å and ~2 GHz for $L=1000$ Å). The angular oscillation frequency was found to be nearly constant at ~58 GHz, independent of the DWNT length. In addition, sustained high-frequency angular motion can be maintained for sufficiently long DWNT (on the order of a few nanometers). For shorter DWNTs, the angular motion can be altered by interference with the axial motion, and becomes irregular. © *2010 American Institute of Physics*.
[doi:10.1063/1.3359654]

I. INTRODUCTION

Carbon nanotubes have exceptional electrical and mechanical properties, such as remarkably high strength coupled with extreme flexibility and low weight. Soon after their discovery by Iijima[1,2] it became clear that these unique properties opened new ranges of applications in nanomechanics.[3] Experiments by Cumings and Zettl[4] showed that double-walled carbon nanotubes (DWNTs) may be employed as gigahertz oscillators when the core is partially pulled out of the outer shell and then released. The force driving the oscillation is an excess van der Waals interaction that is established between the inner and outer tubes. Sustained high-frequency oscillations are possible because the effective friction, arising from dissipation of core kinetic energy into other degrees of freedom, is small when compared to the restoring van der Waals force, as demostrated by experiments[4–7] and confirmed by molecular dynamics (MD) simulations.[8–10] The role of damping on the oscillatory behavior of DWNTs was extensively studied by Rivera *et al.*[11,12] and shown to be significant only on a time scale large compared to typical periods of oscillation. While the maximum and optimum sizes of fullerenes inside nanotubes were calculated by Hodak and Girifalco,[13] their applications in tribology and as fast mechanical oscillators have also received increasing attention.[14,15]

A detailed model of the atomic interactions governing the oscillation behavior of a DWNT should include both covalent bonds between the atoms in each tube as well as van der Waals interaction forces between atoms in the inner and outer tubes. However, some reasonable approximations can be made when studying the oscillation characteristics of DWNTs, and thus permit simple mechanical modeling of these extremely high-frequency systems. First, since covalent bonds are much stiffer than van der Waals interactions, nanotubes can be modeled as rigid bodies in a first approximation.[11] Second, since it was suggested[8] that sustained oscillations are possible independent of tube type when the radial distance between the tubes is ≈3.4 Å, dissipative forces may be neglected, allowing the derivation from a potential of the interaction force between the nanotubes. The Lennard–Jones (LJ) potential was used[16–19] to model the van der Waals interaction in a DWNT system and is adopted in this work. Finally it can be assumed that when the lengths of the nanotubes are large compared to their diameters, the two tubes in a DWNT move coaxially, relative to each other.

With these considerations, the DWNT can be described in first approximation as a system of two rigid tubes moving coaxially under the effect of a LJ potential between their atoms. When the outer shell is fixed the only degrees of freedom of this system are the axial displacement and the axial rotation of the inner tube with respect to the outer tube. In this work, a study of the coupled motion in the axial and angular directions is performed by MD simulations, with particular emphasis on how the respective frequencies change as a function of the DWNT length. The equations of motion that describe the simplified dynamics of a DWNT will be presented next in Sec. II. Details of the MD computational method, including the geometry and boundary conditions are given in Sec. III. We proceed to show simulation results for the oscillation of the DWNT, delineating the nature of axial, angular, and coupled oscillations in Sec. IV. Finally, conclusions of the study are given in Sec. V.

II. EQUATIONS OF MOTION

The equations of motion of the system illustrated in Fig. 1 can be derived by vanishing the variation in the total Hamiltonian H

[a]Electronic address: giacomo@seas.ucla.edu and ghoniem@ucla.edu.

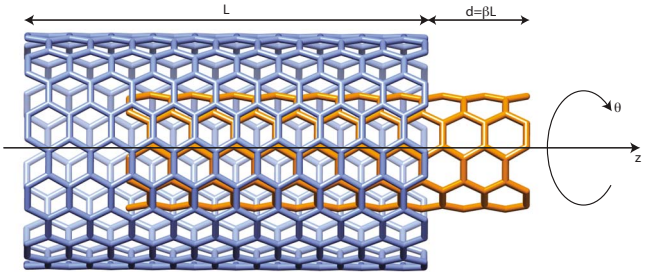

FIG. 1. (Color online) Schematic representation of a DWNT. The present model assumes that the outer tube is fixed and rigid while the inner tube is rigid, and coaxial with respect to the outer tube. The axial displacement z and the rotation angle θ along the DWNT axis define the position of the inner tube atoms. The inner and outer tubes are assumed to have the same length L.

$$\delta H = \delta(T+U) = 0, \tag{1}$$

with T and U being the total kinetic and potential energy of the system, respectively. The total potential energy is calculated as the sum extended over the total number N_T of atoms in the system, with interactions governed by the interatomic potential u_{ij} between two generic atoms

$$U = \frac{1}{2}\sum_{k=1}^{N_T}\sum_{j=1}^{N_T} u_{ij}. \tag{2}$$

Since the total number of atoms is $N_T=N_o+N_i$ with N_o and N_i the number of atoms in the outer and inner tubes, respectively, Eq. (2) can be rewritten in a more convenient form as:

$$U = \frac{1}{2}\sum_{i=1}^{N_o}\sum_{j=1}^{N_o} u_{ij} + \frac{1}{2}\sum_{i=1}^{N_i}\sum_{j=1}^{N_i} u_{ij} + \sum_{i=1}^{N_i}\sum_{j=1}^{N_o} w(d_{ij}^2)$$
$$= U_o + U_i + U_{oi}. \tag{3}$$

The first and second terms in Eq. (3) represent the energies stored in the bonds of the outer and inner tubes, respectively. The third term represents the energy associated with the van der Waals interaction between the two tubes and it is well represented[16] as a LJ potential. The LJ potential between two atoms located respectively at $\boldsymbol{x}_i$ and $\boldsymbol{x}_j$ is a function of their squared distance $d_{ij}^2=\boldsymbol{d}_{ij}\cdot\boldsymbol{d}_{ij}$, where $\boldsymbol{d}_{ij}=\boldsymbol{x}_i-\boldsymbol{x}_j$. It can be expressed in the form:

$$w(d_{ij}^2) = 4\epsilon\left[\left(\frac{d_0^2}{d_{ij}^2}\right)^6 - \left(\frac{d_0^2}{d_{ij}^2}\right)^3\right], \tag{4}$$

where ϵ and d_0 are constants. The total kinetic energy of the DWNT system T is given by

$$T = \frac{1}{2}m_c\sum_{j=1}^{N_T} v_j^2 = \frac{1}{2}m_c\sum_{j=1}^{N_o} v_j^2 + \frac{1}{2}m_c\sum_{j=1}^{N_i} v_j^2 = T_o + T_i, \tag{5}$$

m_c being the mass of a carbon atom. With these notations, the variation in the Hamiltonian reads

$$\delta(T_i+U_{oi}) + \delta T_o + \delta U_o + \delta U_i = 0. \tag{6}$$

Let's now consider the implications of the assumptions considered in this model. First, since the outer tube is fixed, and rigid then $T_o=0$ and $\delta U_o=0$ because there is no variation in the positions of the outer tube atoms. Second, since the inner tube is modeled as being rigid, then $\delta U_i=0$, since there is no relative change in the positions of its atoms. Finally, rigidity and the assumption of coaxial motion allow to express T_i by König theorem in the form $T_i=\frac{1}{2}J_i\dot{\theta}^2+\frac{1}{2}M_i\dot{z}^2$. The total mass M and mass moment of inertia J_i can be written as $M_i=N_im_c$ and $J=M_ir_i^2$ for an inner tube of radius r_i containing N_i atoms. Combining the previous considerations, Eq. (6) becomes

$$\delta\left(\frac{1}{2}N_im_cr_i^2\dot{\theta}^2 + \frac{1}{2}N_im_c\dot{z}^2 + U_{oi}\right) = 0, \tag{7}$$

from which the following associated equations of motion can be derived:

$$Nm_cr^2\ddot{\theta} = -\frac{\partial}{\partial\theta}\sum_{i=1}^{N_i}\sum_{j=1}^{N_o} w(d_{ij}^2)$$
$$Nm_c\ddot{z} = -\frac{\partial}{\partial z}\sum_{i=1}^{N_i}\sum_{j=1}^{N_o} w(d_{ij}^2). \tag{8}$$

The dependence of d_{ij}^2 on the degrees of freedom θ and z can be introduced considering that positions of atoms in the outer tube are fixed and therefore $\boldsymbol{x}_j=\bar{\boldsymbol{x}}_j$. Moreover, positions of atoms in the inner tube can be expressed by the rototranslation $\boldsymbol{x}_i=\boldsymbol{\Omega}(\theta)\bar{\boldsymbol{x}}_i+z\hat{\boldsymbol{z}}$ where $\boldsymbol{\Omega}(\theta)$ and $\hat{\boldsymbol{z}}$ are respectively the orthonormal rotation matrix and the unit axial vector transforming the initial positions $\bar{\boldsymbol{x}}_i$ into the current ones. With these considerations, after applying the chain rule for derivatives, it's finally possible to write the equations of motion in the following form:

$$Nm_cr^2\ddot{\theta} = -2\sum_{i=1}^{N_i}\left(\sum_{j=1}^{N_o} w'\boldsymbol{d}_{ij}\right)\cdot\boldsymbol{\Omega}'\cdot\bar{\boldsymbol{x}}_i$$
$$Nm_c\ddot{z} = -2\sum_{i=1}^{N_i}\left(\sum_{j=1}^{N_o} w'\boldsymbol{d}_{ij}\right)\cdot\hat{\boldsymbol{z}}, \tag{9}$$

where w' and $\boldsymbol{\Omega}'$ indicate the total derivatives of $w(d_{ij}^2)$ and $\boldsymbol{\Omega}(\theta)$ with respect to their own argument, respectively.

III. THE DWNT SIMULATION CELL

The initial configuration of the atoms in a nanotube can be obtained by rolling up a graphene sheet along one on the discrete directions $m\mathbf{a}_1+n\mathbf{a}_2$ in the graphene plane, as illustrated in Fig. 2. The carbon-carbon bond length σ and the chiral indices (m,n) define a cylindrical cell of radius and height respectively:

$$r = \frac{\sqrt{3}\sigma}{2\pi}\sqrt{m^2+mn+m^2}, \tag{10}$$

$$h = \left|(m'-m)\mathbf{a}_1 + (n'-n)\mathbf{a}_2\right|, \tag{11}$$

where

$$m' = m - (m+2n)/\mathrm{GCD}(m+2n, 2m+n),$$

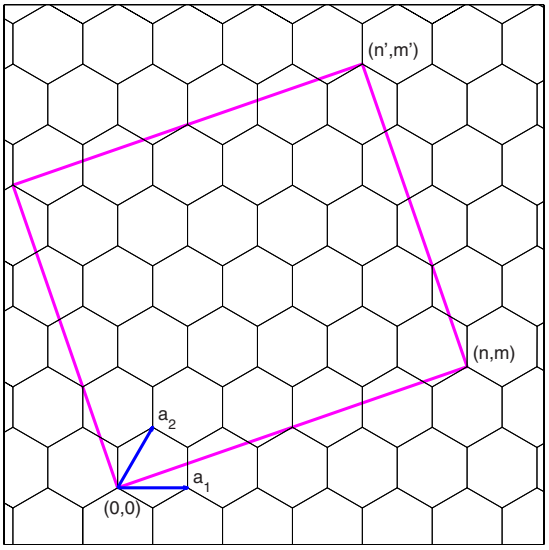

FIG. 2. (Color online) Illustration of an elementary nanotube cell with indices (n,m).

$$n' = n + (2m+n)/\mathrm{GCD}(m+2n, 2m+n), \tag{12}$$

are the chiral indices of the vertex opposite to (0, 0) and GCD indicates the greatest common divisor operator. Nanotubes of $(m,0)$-type are called *zigzag* while the (m,m)-type are called *armchair*.

A DWNT defined by the pair $(m,n)/(M,N)$ of chiral indices of the inner and outer tube is axially commensurate when $m/n=M/N$, otherwise it is said to be axially incommensurate. Commensurability plays an important role in the rotational dynamics of DWNTs because it affects the angular periodicity of the interaction energy. Since angular oscillations are expected to be significant only in DWNT with high degree of commensurability and angular symmetry, it possible to narrow the choice of the chiral indices based on a few considerations. First, armchair-armchair systems, denoted by $(m,m)/(M,M)$, are expected to have more pronounced angular coupling because their atoms are aligned in narrow bands along the axial direction. Second, since the inner and outer tubes in an armchair system have angular periodicity π/m and π/M, respectively, then the DWNT has angular periodicity $\pi\mathrm{GCD}(M,m)/Mm$,[20] which is minimized by taking $M=2m$. For this choice, by using a radial distance between the tubes of ≈3.4 Å (as suggested by experiments,[4] theoretical predictions,[13] and MD simulations[8]) in Eq. (10), the choice of the (5, 5)/(10, 10) DWNT is a natural one for our analysis. Effective friction forces were also found to be particularly low for this configuration,[8,21] hence strengthening our assumption of conservative motion. Table I summarizes the main characteristics of the DWNT analyzed in this paper.

A series of MD simulations is used to analyze the frequency behavior of the (5, 5)/(10, 10) DWNT. With reference to Fig. 1, the outer layer is assumed fixed and the inner layer is assumed to move as a rigid body coaxially, relative to the outer one. Free boundary conditions apply and no cut-off distance is employed for the LJ potential. The time integration method used for the equations of motion is a standard velocity Verlet algorithm, with a time step of 0.1 ps. Such large value of the time-step compared to traditional MD of typical atomic crystals is possible because of the relatively high mass and moment of inertia of the rigid core and weak restoring forces.

TABLE I. Physical properties of the DWNT.

	Inner tube	Outer tube
Chiral indices	(5,5)	(10,10)
Radius[Å]	3.39	6.78
N atoms (L=25 Å)	200	400
N atoms (L=50 Å)	400	800
N atoms (L=100 Å)	820	1640
N atoms (L=1000 Å)	8140	16280
Mass of C	eV ps^2 Å^{-2}	1.2437×10^{-3}
C–C bond length	Å	1.42
ϵ	eV	2.964×10^{-3}
d_0	Å	3.4

IV. SIMULATION RESULTS

Three types of simulations were considered: (1) axial oscillations only (angular motion was suppressed); (2) angular oscillations only (axial motion was suppressed); and (3) coupled axial and angular oscillations.

For the case of axial motion only, the time evolution of the axial coordinate z and restoring axial force are shown in Fig. 3, where the inner layer is released from an initial extrusion $d=L/2$. The influence of the DWNT length on the axial frequency f_z was studied by considering four different lengths: 25, 50, 100, and 1000 Å. As reported in previous studies (e.g. Ref. 17) the characteristic feature of the axial motion is that its frequency decreases with increasing length. In fact when long range effects are negligible, as in the case of van der Waals interactions, the net force on the atoms of the inner tube vanishes due to opposite contributions as long

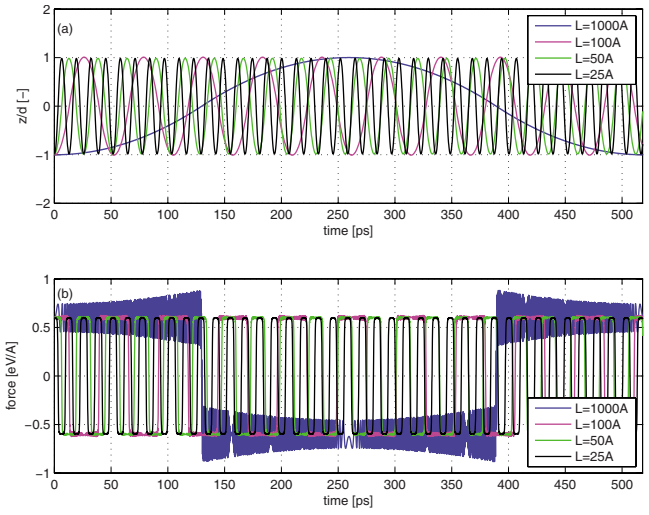

FIG. 3. (Color online) Axial oscillations of (5, 5)/(10, 10) DWNTs for different lengths. (a) Evolution of the axial coordinate z normalized to the extrusion distance $d=L/2$. (b) Evolution of the restoring force: the average value of ≈0.59 eV/Å, independent of the DWNT length, is consistent with previous results (Ref. 9) for the same DWNT configuration.

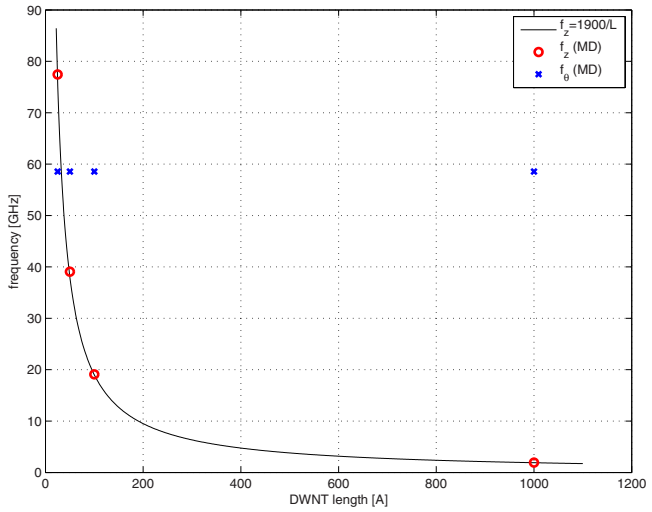

FIG. 4. (Color online) Comparison of axial and angular frequencies for uncoupled motions.

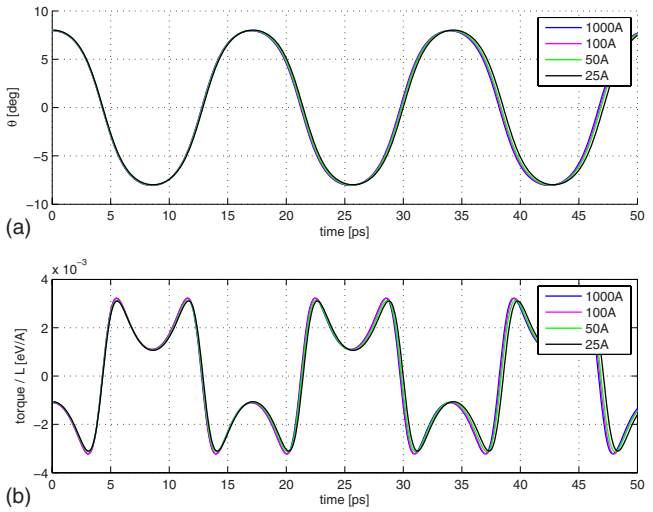

FIG. 5. (Color online) Angular oscillations of (5, 5)/(10, 10) DWNTs for different lengths. (a) Evolution of the angular coordinate θ. (b) Evolution of the restoring torque: the torque magnitude scales as L.

as they are within the ends of the outer tube. Hence, the net average force on the inner shell is due to end effects and is independent of the DWNT length. Using the value of the average restoring force $F_z=0.59$ eV/Å it is possible to estimate the axial period of oscillation T_z by writing

$$\frac{1}{2}\frac{F_z}{M_i}\left(\frac{T_z}{4}\right)^2 = d. \tag{13}$$

For a mass per unit length $m_i=1.0198$ [eV ps^2 Å^{-3}] and an extrusion distance $d=\beta L$ we obtain ($\beta=1/2$)

$$f_z = \frac{1}{4L}\sqrt{\frac{F_z}{2m_i\beta}} \approx \frac{1900\ \text{[GHz Å]}}{L}. \tag{14}$$

A plot of Eq. (14) and a comparison with the results from our MD simulations are shown in Fig. 4.

The high-frequency component of the restoring force is due to the axial corrugation of the interaction energy and increases with length of the DWNT and with z approaching zero (more overlapping for the same DWNT length).

For the case of angular oscillations alone, shown in Fig. 5, the inner tube was constrained at $z=0$ and only the degree of freedom θ was allowed freely to evolve starting from a position near maximum interaction energy. The characteristic of angular oscillations is that their frequency f_θ do not exhibit dependence on the length of the DWNT. In fact in this case not the restoring torque but the restoring torque per unit length is constant. From our simulation results the uncoupled angular frequency is $f_\theta \approx 58.6$ [GHz] and is higher than the axial frequency for $L>33$ Å. The maximum amplitude of the angular oscillation is $\pi \text{GCD}(M,m)/Mm=\pi/m=18°$, for $M=2m=10$.

When both degrees of freedom are let free to evolve coupling of the axial and angular motion is developed. It should be noted, for example, that constant angular frequency is achieved only if displacement in the axial direction are small compared to the DWNT length because the restoring torque is proportional to the overlapping length. In order to preserve constant angular frequency we limit our analysis to the case of small β and consider two regimes, $f_z \ll f_\theta$ and $f_z \approx f_\theta$, respectively. For the first case we choose, $\beta=0.1$ and using Eq. (14) we pick a DWNT of length

$$L_1 = 1000\ \text{Å} \gg \frac{1}{4f_\theta}\sqrt{\frac{F_z}{2m_i\beta}} \approx 73\ \text{Å}. \tag{15}$$

For the second case we choose $\beta \approx 0.05$ and a length

$$L_2 = \frac{1}{4f_\theta}\sqrt{\frac{F_z}{2m_i\beta}} \approx 100\ \text{Å}. \tag{16}$$

Figure 6 shows the results of the MD simulations for the two cases. When the axial motion of the inner shell is slow compared to the uncoupled rotational frequency ($f_z \ll f_\theta$) the two vibration modes are independent, even in the presence of non negligible axial displacement ($\beta L=100$ Å). On the other hand, at comparable frequencies the angular motion becomes largely affected by the axial motion and unstable, even for small axial displacements ($\beta L=5$ Å).

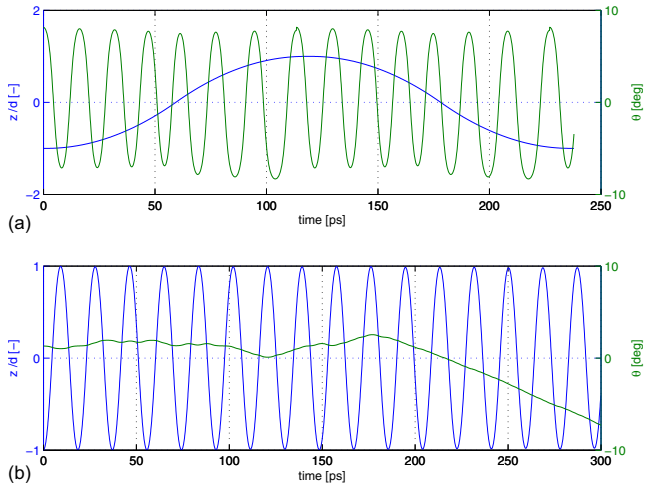

FIG. 6. (Color online) Coupled axial and angular oscillations of (5, 5)/(10, 10) DWNT. (a) Case $f_z \ll f_\theta$: angular oscillations are almost unaffected by the axial motion. (b) Case $f_z \approx f_\theta$: angular oscillations are completely suppressed by the axial motion.

V. CONCLUSIONS

Coupled axial and angular oscillations of a (5, 5)/(10, 10) armchair DWNT were studied for lengths in the range 25–1000 Å using the MD simulation technique. The forces between atoms in the inner and outer tubes were represented with a LJ interatomic potential.

When only axial oscillations were considered, the oscillation frequency turned out to be a decreasing function of the DWNT length. The frequency decreases because the mass increases linearly with length while the restoring force, due to end effects, is independent of the length. The 25 Å nanotube oscillates at an axial frequency of ~78 GHz. As the tube length was increased keeping the initial extrusion ratio $\beta=d/L$ constant, the axial frequency followed the expected $1/L$ law, reaching the value of 2 GHz for the 1000 Å nanotube

When only angular motion was considered, the resulting oscillation frequency was constant, at ~58 GHz, independent of the DWNT length. This can be explained by observing that the restoring torque is not due to end effects; therefore, both restoring torque and moment of inertia scale proportionally with length of the inner tube, resulting in a length independent equation of motion governing the angular degree of freedom. For sufficiently long nanotubes, the angular frequency is higher than the axial frequency: for the (5, 5)/(10, 10) armchair DWNT with $\beta=1/2$ this happens at $L \approx 33$ Å. The maximum amplitude of the angular oscillation is governed by the angular periodicity of the DWNT, which in our case is 18°. It should be noticed that such high angular frequencies are still much smaller than the critical speed of nanotube collapse reported in previous studies.[22]

The coupled motion reveals a strong dependence on the (5, 5)/(10, 10) DWNT length. For short DWNTs (in the subnanometer range) the axial and angular frequencies are comparable and a regular angular motion cannot be sustained. For longer DWNT the angular and axial motion decouple and a sustained periodic angular oscillation is observed. When the axial vibration is small compared to the axial length ($\beta \ll 1$), full amplitude and constant high-frequency rotational oscillations can be obtained.

ACKNOWLEDGMENTS

This work was supported by the National Science Foundation under Grant Nos. 0506841 and 0625299 with UCLA.

[1] S. Iijima, Nature (London) **354**, 56 (1991).
[2] S. Iijima, Nature (London) **363**, 603 (1993).
[3] S. Sinnott and R. Andrews, Crit. Rev. Solid State Mater. Sci. **26**, 145 (2001).
[4] J. Cumings and A. Zettl, Science **289**, 602 (2000).
[5] M.-F. Yu, O. Lourie, M. J. Dyer, K. Moloni, T. F. Kelly, and R. Ruoff, Science **287**, 637 (2000).
[6] M.-F. Yu, B. I. Yakobson, and R. Ruoff, J. Phys. Chem. B **104**, 8764 (2000).
[7] A. Kis, K. Jensen, S. Aloni, W. Mickelson, and A. Zettl, Phys. Rev. Lett. **97**, 025501 (2006).
[8] S. B. Legoas, V. R. Coluci, S. F. Braga, P. Z. Coura, S. O. Dantas, and D. S. Galvao, Phys. Rev. Lett. **90**, 055504 (2003).
[9] W. Guo, Y. Guo, H. Gao, Q. Zheng, and W. Zhong, Phys. Rev. Lett. **91**, 125501 (2003).
[10] P. Tangney, S. G. Louie, and M. L. Cohen, Phys. Rev. Lett. **93**, 065503 (2004).
[11] J. L. Rivera, C. McCabe, and P. T. Cumming, Nano Lett. **3**, 1001 (2003).
[12] J. L. Rivera, C. McCabe, and P. T. Cumming, Nanotechnology **16**, 186 (2005).
[13] M. Hodak and L. A. Girifalco, Chem. Phys. Lett. **350**, 405 (2001).
[14] C.-C. Ma, Y. Zhao, C.-Y. Yam, G. H. Chen, and Q. Jiang, Nanotechnology **16**, 1253 (2005).
[15] B. J. Cox, N. Thamwattana, and J. M. Hill, Proc. R. Soc. London, Ser. A **463**, 477 (2007).
[16] L. A. Girifalco, M. Hodak, and R. S. Lee, Phys. Rev. B **62**, 13104 (2000).
[17] Q. Zheng and Q. Jiang, Phys. Rev. Lett. **88**, 045503 (2002).
[18] Q. Zheng, J. Z. Liu, and Q. Jiang, Phys. Rev. B **65**, 245409 (2002).
[19] D. Baowan and J. Hill, Z. Angew. Math. Phys. **58**, 857 (2007).
[20] R. C. Merkle, Nanotechnology **4**, 86 (1993).
[21] P. Liu, Y. W. Zhang, and C. Lu, J. Appl. Phys. **98**, 014301 (2005).
[22] S. Zhang, W. K. Liu, and R. S. Ruoff, Nano Lett. **4**, 293 (2004).